FEBS Letters 587 (2013) 1736–1741

FEBS Letters

journal homepage: www.FEBSLetters.org

A Trp199Glu MauG variant reveals a role for Trp199 interactions with pre-methylamine dehydrogenase during tryptophan tryptophylquinone biosynthesis

Nafez Abu Tarboush [a], Lyndal M.R. Jensen [b], Carrie M. Wilmot [b], Victor L. Davidson [c,*]

[a] Biochemistry and Physiology Department, College of Medicine, The University of Jordan, Amman 11942, Jordan
[b] Department of Biochemistry, Molecular Biology and Biophysics, University of Minnesota, Minneapolis, MN 55455, United States
[c] Burnett School of Biomedical Sciences, College of Medicine, University of Central Florida, Orlando, FL 32827, United States

ARTICLE INFO

Article history:
Received 15 April 2013
Revised 27 April 2013
Accepted 29 April 2013
Available online 10 May 2013

Edited by Peter Brzezinski

Keywords:
Electron transfer
Protein–protein interaction
Kinetic mechanism
Cofactor biosynthesis

ABSTRACT

MauG catalyzes posttranslational modifications of a methylamine dehydrogenase precursor (pre-MADH) to complete the biosynthesis of its protein-derived tryptophan tryptophylquinone (TTQ) cofactor. Trp199 is present at the site of interaction between MauG and preMADH and is critical to this process as it mediates hole hopping during the inter-protein electron transfer that is required for catalysis. Trp199 was converted to Glu and the structure and reactivity of the W199E/preMADH complex were characterized. The results reveal that the nature of residue 199 is also important for productive complex formation between preMADH and MauG.

Structured summary of protein interactions:
preMADH light chain, **preMADH heavy chain** and **MauG** physically interact by X-ray crystallography (View interaction).

1. Introduction

MauG is a diheme enzyme [1] that catalyzes the biosynthesis of the protein-derived tryptophan tryptophylquinone (TTQ) cofactor in methylamine dehydrogenase (MADH) [2]. The biosynthetic process is a six-electron oxidation of a preMADH precursor protein with a mono-hydroxylated residue βTrp57 [3]. These catalytic reactions require long range electron transfer (ET) as the crystal structure of the MauG–preMADH complex from *Paracoccus denitrificans* [4] (Fig. 1) showed that the distances between the side-chain of βTrp108 of preMADH and the hemes of MauG were 40.1 and 19.4 Å. The catalytic competence of this structure was confirmed by demonstration that addition of H_2O_2 to MauG–preMADH crystals results in synthesis of the mature TTQ cofactor [4]. The order of the reactions that MauG catalyzes are covalent crosslinking of βTrp57 to βTrp108, insertion of a second oxygen atom into the side-chain of βTrp57, and oxidation of the quinol species to the quinone [5] (Fig. 2A). These reactions proceed via a *bis*-Fe(IV) intermediate of MauG [6] in which one heme is present as Fe(IV)=O with an axial His ligand and the other is Fe(IV) with axial ligands provided by His and Tyr residues [4].

Trp199 of MauG resides at the site of interaction with preMADH and is positioned approximately halfway between βTrp108 and the nearest heme of MauG (Fig. 1). Previously, conversion of Trp199 to Phe or Lys resulted in MauG variants that were unable to catalyze TTQ biosynthetic ET reactions that required the *bis*-Fe(IV) intermediate (Fig. 2A,B), but were still functional in a non-biosynthetic ET reaction from diferrous MauG to the quinone form of MADH [7] (Fig. 2C). On the basis of these studies and subsequent kinetic and thermodynamic analysis of these reactions [8], it was concluded that the ET reaction involving the *bis*-Fe(IV) intermediate (Fig. 2B) occurred via a multistep hole-hopping mechanism, during which Trp199 was reversibly oxidized to a Trp radical allowing it to mediate the hole-hopping reaction, while the non-biosynthetic ET reaction (Fig. 2C) occurred via single-step electron tunneling.

In this study Trp199 was converted to Glu. The W199E mutation does not alter the physical properties of MauG yet it renders the enzyme inactive in the TTQ biosynthetic reactions. It is active in the non-biosynthetic ET reaction between diferrous MauG and quinone MADH. However, the W199E mutation alters the kinetic

Abbreviations: E_m, Oxidation–reduction midpoint potential; ET, electron transfer; MADH, methylamine dehydrogenase; TTQ, tryptophan tryptophylquinone; preMADH, the biosynthetic precursor protein of MADH with incompletely synthesized TTQ; WT, wild-type

* Corresponding author. Address: Burnett School of Biomedical Sciences, College of Medicine, University of Central Florida, 6900 Lake Nona Blvd., Orlando, FL 32827, United States. Fax: +1 407 266 7002.
E-mail address: victor.davidson@ucf.edu (V.L. Davidson).

0014-5793/$36.00
http://dx.doi.org/10.1016/j.febslet.2013.04.047

mechanism of this reaction relative to what was observed with other Trp199 variants and wild-type (WT) MauG. The crystal structure of the W199E MauG–preMADH complex reveals the structural basis for this effect.

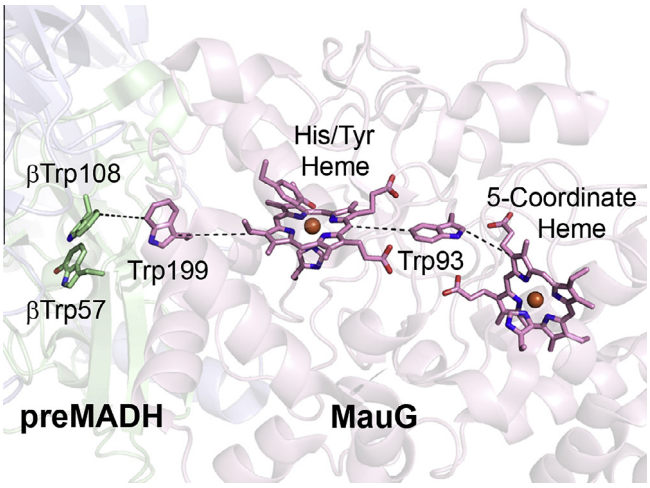

Fig. 1. Positions of hemes and residues involved in hole-hopping mediated ET in the WT MauG/preMADH crystal structure (PDB ID, 3L4M). Hemes and residues are drawn in stick colored by atom, and the remaining protein is drawn in cartoon (MauG, pink; preMADH α-subunit, blue; preMADH β-subunit, green). Irons are represented as orange spheres. Closest atoms between adjacent hemes and residues are joined by dotted lines.

2. Materials and methods

2.1. Protein expression and purification

Trp199 of MauG was converted to Glu by site-directed mutagenesis of pMEG391 [1], which contains *mau*G, using the QuikChange kit (Strategene). Homologous expression of W199E MauG in *P. denitrificans* and purification were as described for recombinant WT MauG [1]. Native WT MADH was purified from *P. denitrificans* [9] and preMADH [3] was expressed in *Rhodobacter sphaeroides* and purified as described previously [10].

2.2. Redox titrations

The oxidation–reduction midpoint potential (E_m) values of W199E MauG were determined by anaerobic spectrochemical titrations, as described previously for native MauG [11]. Data were fit using Eq. (1), which describes the redox behavior of a system with two redox active centers, where a is the fraction of the total absorbance change attributable to one center and $(1-a)$ is the fraction of the total absorbance change attributable to the other.

$$\text{Fraction reduced} = a/[1+10^{((E-Em1)/0.059V)}] + (1-a)/[1+10^{((E-Em2)/0.059V)}] \quad (1)$$

2.3. Assay of MauG-dependent TTQ Biosynthesis

The steady-state kinetic assay of MauG-dependent TTQ biosynthesis from preMADH was performed as previously described

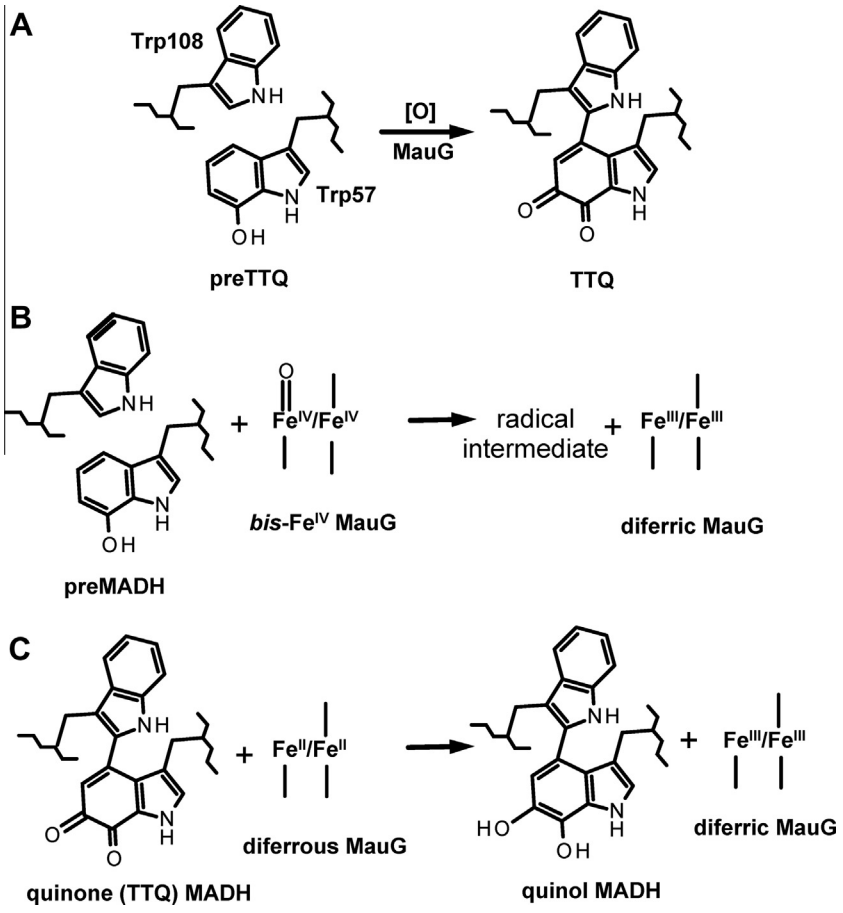

Fig. 2. Reactions of MauG with different forms of MADH and preMADH. (A) Steady-state MauG-dependent TTQ biosynthesis from preTTQ on preMADH. [O] refers to H_2O_2 or O_2 plus a reductant. (B) The initial two-electron oxidation of preMADH by *bis*-Fe(IV) MauG which yields a radical intermediate that is present on preMADH [5]. (C) The non-biosynthetic ET reaction from diferrous MauG to oxidized MADH.

[12,13]. WT or W199E MauG was mixed with preMADH in 0.01 M potassium phosphate buffer, pH 7.5 at 25 °C. Reactions were initiated by addition of 100 μM H_2O_2 and the rate of appearance of quinone MADH was monitored at 440 nm.

2.4. ET from diferrous MauG to quinone MADH

The ET reaction from diferrous W199E MauG to quinone MADH was studied by single-turnover kinetics as described previously for WT MauG [14]. The reaction was monitored by the decrease in absorbance at 550 nm which corresponds to the conversion of diferrous to diferric MauG [1]. Data were analyzed using the kinetic model in Eq. (2), where S is quinone MADH, E is diferrous MauG, E′ is diferric MauG, and P is quinol MADH and data were fit to either Eqs. (3), (4).

$$E + S \underset{k_2}{\overset{k_1}{\rightleftharpoons}} ES \underset{k_4}{\overset{k_3}{\rightleftharpoons}} E'P \quad (2)$$

$$k_{obs} = k_3[S]/([S] + k_d) + k_4 \quad (3)$$

$$k_{obs} = k_1[S] + [k_2k_4/(k_3 + k_4)] \quad (4)$$

2.5. EPR spectroscopy

EPR samples were prepared in 50 mM potassium phosphate buffer, pH 7.4, with 150 μM protein. For the H_2O_2-treated samples, stoichiometric H_2O_2 was added to the enzyme and the reaction mixtures were immediately transferred to quartz EPR tubes and frozen in liquid nitrogen. The total reaction time was 30–40 s. Continuous wave X-band EPR spectra were taken by a Bruker E200 spectrometer at 100-kHz modulation frequency using a dual mode resonator. Temperature was maintained at 10 K with an ESR910 liquid helium cryostat and an ITC503 temperature controller.

2.6. X-ray crystallography

Single crystals were obtained by hanging drop vapor diffusion from drops assembled with 1 μl protein solution (100 μM W199E MauG and 50 μM preMADH in 10 mM potassium phosphate, pH 7.5) layered with 3 μl of reservoir solution (23% w/v PEG 8000, 0.1 M sodium acetate, 0.1 M MES pH 6.4). Crystals were cryoprotected as described previously through inclusion of 10% PEG 400 [4]. X-ray diffraction data were collected at 100 K at GM/CA-CAT beamline 23-ID-D of the Advanced Photon Source, Argonne National Laboratory, Argonne, IL. The diffraction data were essentially isomorphous with data obtained from WT MauG/preMADH crystals, and are in the space group *P*1 with one complex (two W199E MauG bound to one preMADH) in the asymmetric unit. The data were processed with HKL2000 [15].

The structure solutions were obtained by difference Fourier. Refinement was carried out using REFMAC [16] in the CCP4 program suite [17] and model-building was carried out in COOT [18]. The initial model used the coordinates of WT MauG/preMADH complex (PDB entry 3L4M) retaining only the protein and solvent components and with residue 199 of MauG truncated to Ala. Restrained refinement with TLS was carried out using no distance restraints between the heme iron centers and their ligands. Glu199 was well-ordered, and added to the model based on the $2F_o$–F_c and F_o–F_c electron density maps. Refinement was deemed complete when the F_o–F_c electron density contained only noise.

3. Results

3.1. Spectroscopic and redox properties of W199E MauG

The absorption spectra of the diferric and diferrous forms of W199E MauG were essentially the same as that of WT MauG (Fig. 3A,B). The diferric form exhibits a Soret peak maximum at 406 nm. In the spectrum of each diferrous protein the Soret peak maximum shifts to 418 nm and α and β bands appear at 550 and 522 nm, respectively. Spectrochemical titration of W199E MauG yielded two E_m values of −161 ± 4 and −241 ± 8 mV which were similar to those of WT MauG of −158 ± 9 and −246 ± 3 mV [11].

3.2. Effects of the W199E mutation on the formation of bis-Fe(IV) MauG and its reactivity toward preMADH

W199E MauG exhibited no detectable TTQ biosynthesis activity in the steady-state assay with up to 20 μM preMADH as the substrate, whereas WT MauG exhibited a k_{cat} value of 0.2 s^{-1} and K_m value of 6.6 μM for preMADH [19]. The spectroscopic features of the *bis*-Fe(IV) redox state of MauG, which is an intermediate in the TTQ biosynthetic reactions, have been previously characterized [6,19]. The *bis*-Fe(IV) formation is accompanied by a decrease in intensity and small shift of the Soret peak in the absorption spectrum of MauG. These same spectral changes were observed upon reaction of diferric W199E MauG with H_2O_2 (Fig. 3C,D). The EPR spectrum of diferric W199E MauG includes signals of high-spin and low-spin hemes exhibiting *g* values that are very similar to that of WT MauG [1] (Fig. 4). A significant decrease in the intensity of both signals following addition of H_2O_2 is observed in the EPR spectrum of W199E MauG, consistent with conversion to the EPR-silent *bis*-Fe(IV) state, as also observed for WT MauG (Fig. 4) [6]. Addition of preMADH to WT *bis*-Fe(IV) MauG converts MauG back to the diferric state. This reaction exhibits a rate of 0.8 s^{-1}, and a K_d < 1.5 μM [19]. In contrast, no reaction was observed on addition of up to 20 μM preMADH to *bis*-Fe(IV) W199E MauG.

3.3. Effects of the Trp199 mutation on the ET reaction from diferrous MauG to quinone MADH

Although not involved in TTQ biosynthesis, a thermodynamically favorable ET reaction from diferrous MauG to quinone MADH has been characterized [14] (Fig. 2C). As this reaction does not involve the formation of the *bis*-Fe(IV) species, it has been used to distinguish mutations of MauG that destabilize the *bis*-Fe(IV) state from those that disrupt ET between the two proteins [7,20], and to distinguish whether mutations which affect ET do so by affecting the hole-hopping mediated ET to the *bis*-Fe(IV) species or the single-step electron tunneling between TTQ of MADH and the hemes of MauG [7,8]. The reaction of WT MauG exhibited a hyperbolic dependence of the rate on [MADH] (saturation behavior) with a limiting first-order rate constant of 0.07 s^{-1} and K_d value of 10.1 μM. The reactions with previously described W199F and W199K MauG variants also exhibited saturation behavior and reaction rates similar to WT MauG [7]. In contrast, W199E MauG exhibited a linear dependence on [MADH] (Fig. 5) with a bimolecular rate constant of 170 ± 10 M^{-1} s^{-1}. These results indicate that mutation of Trp199, specifically to Glu, altered the kinetic mechanism for this interprotein ET reaction, such that the binding step is now slower than the ET rate (i.e., $k_1[S] + k_2 \ll k_3$, in Eq. (2)).

3.4. X-ray crystal structure of the W199E MauG/preMADH complex

W199E MauG was co-crystallized with preMADH and the X-ray crystal structure solved to a resolution of 1.93 Å. Data collection and refinement statistics are given in Table 1. The W199E-MauG/preMADH complex (PDB entry 3RN1) has the same overall structure as that of the WT MauG/preMADH complex (PDB entry 3L4M), with two crystallographically independent copies of W199E MauG in the asymmetric unit (RMSD values on Cα positions in the range of 0.15–0.32 Å). The positions of the nascent

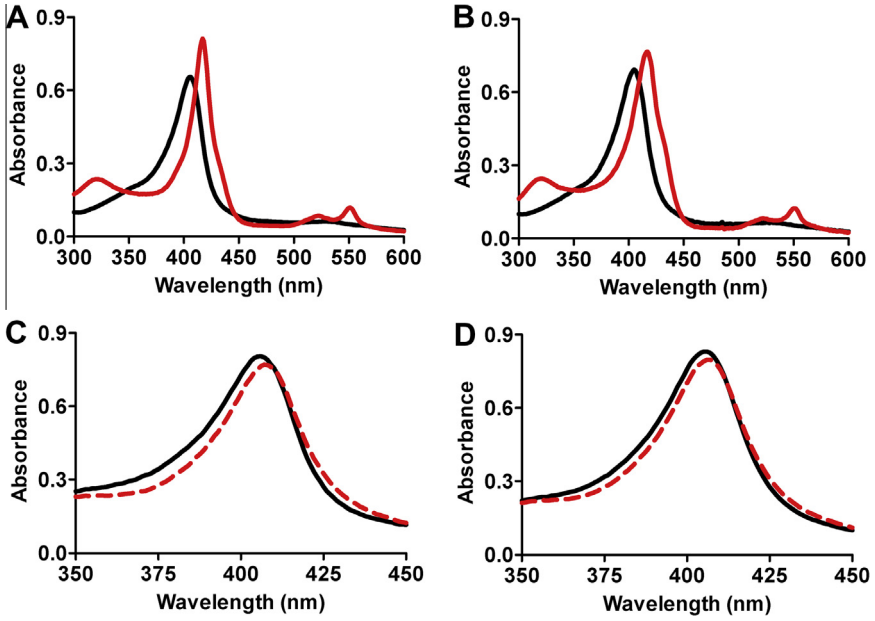

Fig. 3. Comparison of the spectra of different redox states of MauG and W199E MauG. The spectra of diferric (black) and diferrous (red) forms of native MauG (A) and W199E MauG (B) are overlaid. The spectra of the diferric proteins before (black) and after (red) addition of H_2O_2, which forms the *bis*-Fe(IV) redox state, are shown for native MauG (C) and W199E MauG (D).

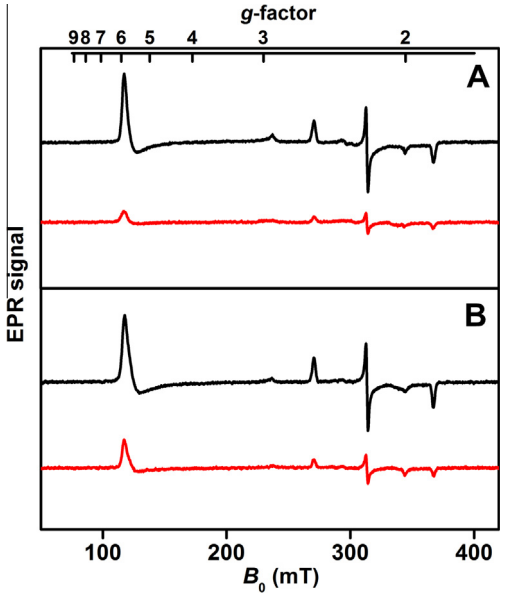

Fig. 4. EPR spectra of (A) native MauG and (B) W199E MauG. In each panel the black upper spectrum is the diferric enzyme and the red lower spectrum is the enzyme after addition of 1 equiv of H_2O_2. EPR parameters for obtaining spectra are as follows: temperature, 10 K; microwave, 1 mW at 9.44 GHz; modulation amplitude, 0.5 mT.

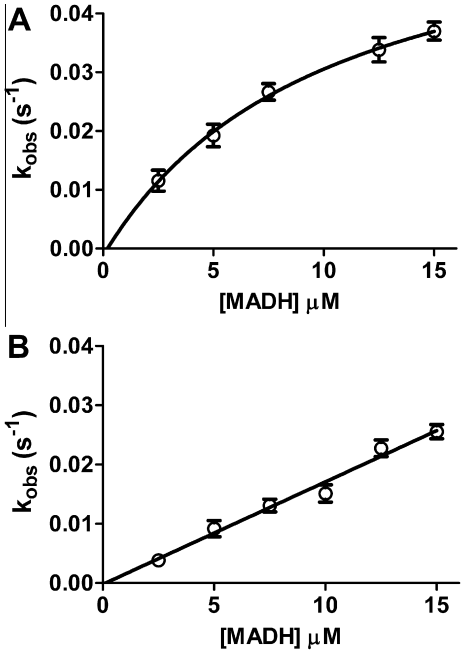

Fig. 5. Reaction of the quinone form of MADH with diferrous native MauG (A) and W199E MauG (B). The lines are fits of the data by Eq. (3) in A and Eq. (4) in B. Each data point is the average of four replicates with the error bars included.

TTQ sites, both hemes and the intervening Trp93 residue are preserved in W199E MauG.

The position of Glu199 at the interface of MauG and preMADH is essentially the same as that of the native Trp199 residue (Fig. 6A). In the WT MauG/preMADH crystal structure, Glu101 of the preMADH β-subunit is the only preMADH residue that directly contacts Trp199, whose indole nitrogen forms a weak hydrogen bond with the side chain of βGlu101 (3.2 Å) (Fig. 6B). In the W199E MauG/preMADH structure Glu199 sits close to βGlu101 (4.6 Å between the two closest side chain oxygens) with an ordered water mediating interaction between the side chains (Fig. 6B). In the WT MauG/preMADH structure the only other protein contacts the Trp199 side chain makes are with other MauG residues, with one face of the indole ring being packed against the side chains of Val195, Leu334 and Arg338. In the W199E MauG/preMADH structure, these three residues are superimposable with those of the WT complex, with the only interaction in the mutant being between Val195 and the Cγ of Glu199. Other than this, the Glu199 side chain makes no direct contacts with any other protein residue within the interface.

Table 1
X-ray crystallography data collection and refinement statistics.[a].

Data collection	W199E MauG/preMADH
Detector type	MAR*mosaic* 4 × 4 tiled CCD
Source	APS, Sector 23
Space group	*P*1
Unit cell lengths (Å)[b]	55.53 × 83.52 × 107.78
Unit cell angles (°)[b]	109.94, 91.54, 105.78
Wavelength (Å)	1.03315
Resolution (Å)	50.00–1.93 (1.96–1.93)
Measured reflections	500,045
Unique reflections	126,588
Completeness (%)[c]	97.5 (93.3)
R_{merge} (%)[d]	9.2 (32.3)
$I/\sigma I$	13.0 (3.8)
Multiplicity	4.0 (3.6)
Refinement	
Resolution (Å)	43.46–1.93 (1.98–1.93)
No. reflections; working/test	113, 977/6, 302
R_{work} (%)[e]	14.4
R_{free} (%)[f]	19.2
Protein atoms	13,309
Ligand atoms	215
Solvent sites	1,390
Ramachandran statistics[g]	
Allowed (%)	99.17
Outliers (%)	0.83
Root mean square deviation	
Bond lengths (Å)	0.024
Bond angles (°)	2.017
Average B-factor (Å^2)	17.69
ESU (Å)[h]; R_{work}/R_{free}	0.141/0.134
PDB code	3RN1

[a] Values in parentheses are for the highest resolution shell.
[b] The cell constants for the native W199E-MauG/preMADH structures were isomorphous with WT MauG/preMADH, and therefore set to those of PDB entry 3L4M.
[c] Values for the highest resolution shell are given in parentheses.
[d] $R_{merge} = \Sigma_i|I_{hkl,i} - \langle I_{hkl}\rangle|/\Sigma_{hkl}\ \Sigma_i\ I_{hkl,i}$, where I is the observed intensity and $\langle I_{hkl}\rangle$ is the average intensity of multiple measurements.
[e] $R_{work} = \Sigma||F_o| - |F_c||/\Sigma|F_o|$, where $|F_o|$ is the observed structure factor amplitude, and $|F_c|$ is the calculated structure factor amplitude.
[f] R_{free} is the R factor based on 5% of the data excluded from refinement.
[g] Based on values attained from refinement validation options in COOT.
[h] Estimated standard uncertainties generated for R_{work} and R_{free} in Refmac5.5 in the CCP4i suite.

4. Discussion

It was previously established that Trp199 of MauG is critical to TTQ biosynthesis, as it is reversibly oxidized to a Trp radical while mediating hole-hopping from preMADH to *bis*-Fe(IV) MauG during the long-range ET required for catalysis [7,8]. W199F and W199K MauG variants were unable to mediate hole-hopping, but the presence of Phe or Lys did not affect complex formation between preMADH and MauG, and these residues could support an electron tunneling reaction that did not require hopping. Those results suggested that residue 199 affected TTQ biosynthesis solely through provision of a hopping intermediate during ET. However, the results obtained for W199E MauG indicate that this mutation also affects the kinetics of complex formation that precedes the interprotein ET, such that the rate of formation of the complex in an orientation optimized for ET is now rate-limiting for the electron tunneling reaction from diferrous MauG to oxidized MADH. The crystal structure of the W199E MauG/preMADH complex provides an explanation for this phenomenon.

In the WT MauG/preMADH complex the only direct interaction that Trp199 makes with the β-subunit of preMADH is a hydrogen bond with βGlu101 of preMADH (Fig. 6B). Replacement of Trp199 with Glu brings this acidic residue in close proximity to βGlu101. The crystal structure of W199E MauG/preMADH shows that the hydrogen bonds are short between the two glutamate side chains and the intervening water, and the closest O of the two glutamates are only 4.6 Å apart (Fig. 6B). Although the pK_a of the two glutamates are unknown, the high solvation in this part of the interface and the short hydrogen bonds suggest that they both carry a negative charge. Thus, it seems highly likely that there are different conformers of βGlu101 and Glu199 in solution, some of which result in electrostatic repulsion that may interfere with productive binding, reactivity and crystal formation (for example, a 180° rotation about the Cβ–Cγ bond of Glu199). The crystallization has likely selected out the most stable complex from a number of ensembles present in solution. The presence of the other conformers in solution will effectively slow the rate of complex formation as many possible orientations of W199E MauG must be sampled before the complex structure that is optimized for ET is achieved.

The effect of the W199E mutation on the biosynthetic ET reaction (Fig. 2B) is not evident since Glu cannot support the required hopping mechanism, and therefore there was no observable reaction. However, these results demonstrate that residue 199 does play multiple roles in MauG-catalyzed TTQ biosynthesis, not only in mediating a hole-hopping mechanism of interprotein ET but also in facilitating efficient complex formation between preMADH and MauG. These results also illustrate how subtle changes in protein–protein interactions can significantly affect the mechanism and rate of interprotein ET reactions.

Acknowledgements

We thank Dr. Aimin Liu and Jiafeng Geng at Georgia State University for performing the EPR experiments and providing Fig. 4,

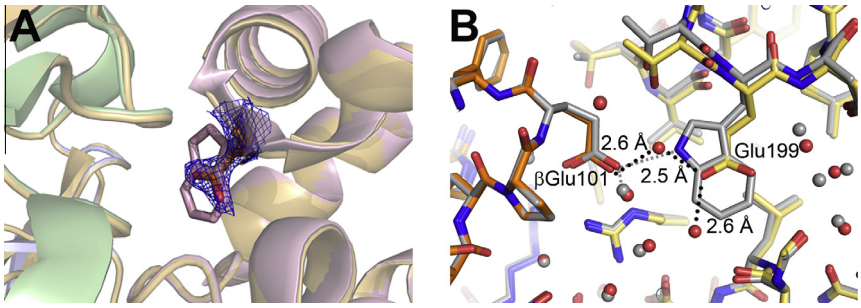

Fig. 6. (A) Overlay of the interface region of the W199E MauG/preMADH and WT MauG/preMADH complexes. W199E MauG/preMADH is drawn in gold cartoon, with the coordinates of the MauG Glu199 side chain drawn as sticks colored by atom (carbon, gold), and the $2F_o$–F_c map drawn as a blue mesh contoured at 1.5 σ. The WT MauG/preMADH is drawn as cartoon (MauG: pink; β-preMADH: green; and α-preMADH: blue). (B) Interface region and hydrogen bonding involving MauG residue 199 and preMADH βGlu101. W199E MauG/preMADH is drawn as sticks colored by atom (carbon: W199E MauG, yellow; preMADH α-subunit, blue; preMADH β-subunit, orange) with waters as red spheres. Hydrogen bonds are drawn as black dotted lines, and lengths indicated. WT MauG/preMADH is drawn as sticks colored by atom (carbon, grey) with waters as grey spheres. Hydrogen bonds in WT MauG/preMADH are drawn as grey dashed lines.

and Yu Tang for technical assistance. This work was supported by NIH Grants GM41574 (VLD) and GM66569 (CMW) and a Minnesota Partnership for Biotechnology and Medical Genomics Grant SPAP-05-0013-P-FY06 (CMW). Computer resources were provided by the Basic Sciences Computing Laboratory of the University of Minnesota Supercomputing Institute. X-ray data were collected at Sector 23, GM/CA-CAT at the Advanced Photon Source (APS), Argonne National Laboratory, Argonne, IL. GM/CA CAT has been funded in whole or in part with Federal funds from the National Cancer Institute (Y1-CO-1020) and the National Institute of General Medical Science (Y1-GM-1104). Use of the APS was supported by the U.S. Department of Energy, Basic Energy Sciences, Office of Science, under contract No. DE-AC02-06CH11357. We thank Ed Hoeffner for Kahlert Structural Biology Laboratory support at The University of Minnesota.

References

[1] Wang, Y., Graichen, M.E., Liu, A., Pearson, A.R., Wilmot, C.M. and Davidson, V.L. (2003) MauG, a novel diheme protein required for tryptophan tryptophylquinone biogenesis. Biochemistry 42, 7318–7325.
[2] Davidson, V.L. (2001) Pyrroloquinoline quinone (PQQ) from methanol dehydrogenase and tryptophan tryptophylquinone (TTQ) from methylamine dehydrogenase. Adv. Protein Chem. 58, 95–140.
[3] Pearson, A.R. et al. (2004) Further insights into quinone cofactor biogenesis: probing the role of mauG in methylamine dehydrogenase tryptophan tryptophylquinone formation. Biochemistry 43, 5494–5502.
[4] Jensen, L.M., Sanishvili, R., Davidson, V.L. and Wilmot, C.M. (2010) In crystallo posttranslational modification within a MauG/pre-methylamine dehydrogenase complex. Science 327, 1392–1394.
[5] Yukl, E.T., Liu, F., Krzystek, J., Shin, S., Jensen, L.M., Davidson, V.L., Wilmot, C.M. and Liu, A. (2013) Diradical intermediate within the context of tryptophan tryptophylquinone biosynthesis. Proc. Natl. Acad. Sci. USA 110, 4569–4573.
[6] Li, X., Fu, R., Lee, S., Krebs, C., Davidson, V.L. and Liu, A. (2008) A catalytic di-heme bis-Fe(IV) intermediate, alternative to an Fe(IV)═O porphyrin radical. Proc. Natl. Acad. Sci. USA 105, 8597–8600.
[7] Abu Tarboush, N., Jensen, L.M.R., Yukl, E.T., Geng, J., Liu, A., Wilmot, C.M. and Davidson, V.L. (2011) Mutagenesis of tryptophan199 suggets that hopping is required for MauG-dependent tryptophan tryptophylquinone biosynthesis. Proc. Natl. Acad. Sci. USA 108, 16956–16961.
[8] Choi, M., Shin, S. and Davidson, V.L. (2012) Characterization of electron tunneling and hole hopping reactions between different forms of MauG and methylamine dehydrogenase within a natural protein complex. Biochemistry 51, 6942–6949.
[9] Davidson, V.L. (1990) Methylamine dehydrogenases from methylotrophic bacteria. Methods Enzymol. 188, 241–246.
[10] Graichen, M.E., Jones, L.H., Sharma, B.V., van Spanning, R.J., Hosler, J.P. and Davidson, V.L. (1999) Heterologous expression of correctly assembled methylamine dehydrogenase in *Rhodobacter sphaeroides*. J. Bacteriol. 181, 4216–4222.
[11] Li, X., Feng, M., Wang, Y., Tachikawa, H. and Davidson, V.L. (2006) Evidence for redox cooperativity between *c*-type hemes of MauG which is likely coupled to oxygen activation during tryptophan tryptophylquinone biosynthesis. Biochemistry 45, 821–828.
[12] Li, X., Jones, L.H., Pearson, A.R., Wilmot, C.M. and Davidson, V.L. (2006) Mechanistic possibilities in MauG-dependent tryptophan tryptophylquinone biosynthesis. Biochemistry 45, 13276–13283.
[13] Feng, M., Jensen, L.M., Yukl, E.T., Wei, X., Liu, A., Wilmot, C.M. and Davidson, V.L. (2012) Proline 107 is a major determinant in maintaining the structure of the distal pocket and reactivity of the high-spin heme of MauG. Biochemistry 51, 1598–1606.
[14] Shin, S., Abu Tarboush, N. and Davidson, V.L. (2010) Long-range electron transfer reactions between hemes of MauG and different forms of tryptophan tryptophylquinone of methylamine dehydrogenase. Biochemistry 49, 5810–5816.
[15] Otwinowski, Z. and Minor, W. (1997) Processing of X-ray diffraction data collected in oscillation mode. Methods Enzymol. 276, 307–326.
[16] Murshudov, G.N., Vagin, A.A. and Dodson, E.J. (1997) Refinement of macromolecular structures by the maximum-likelihood method. Acta Crystallogr. D Biol. Crystallogr. 53, 240–255.
[17] Winn, M.D. et al. (2011) Overview of the CCP4 suite and current developments. Acta Crystallogr. D Biol. Crystallogr. 67, 235–242.
[18] Emsley, P. and Cowtan, K. (2004) Coot: model-building tools for molecular graphics. Acta Crystallogr. D Biol. Crystallogr. 60, 2126–2132.
[19] Lee, S., Shin, S., Li, X. and Davidson, V.L. (2009) Kinetic mechanism for the initial steps in MauG-dependent tryptophan tryptophylquinone biosynthesis. Biochemistry 48, 2442–2447.
[20] Abu Tarboush, N., Jensen, L.M., Feng, M., Tachikawa, H., Wilmot, C.M. and Davidson, V.L. (2010) Functional importance of tyrosine 294 and the catalytic selectivity for the bis-Fe(IV) state of MauG revealed by replacement of this axial heme ligand with histidine. Biochemistry 49, 9783–9791.